Interface coupling in a ferromagnet/antiferromagnet bilayer

Marco Finazzi*

INFM and Dipartimento di Fisica del Politecnico di Milano, Piazza Leonardo da Vinci 32, 20133 Milano, Italy

A micromagnetic model accounting for exchange, dipolar interactions, and magnetocrystalline anisotropy has been applied to simulate the magnetic structure of a low anisotropy antiferromagnetic thin film on a ferromagnetic substrate. In particular, the influence that interface uncompensated moments have on the type of magnetic coupling between the antiferromagnetic and ferromagnetic layers has been evaluated. The long-range magnetic dipole-dipole interactions force the antiferromagnetic film to have in-plane anisotropy. For the fully magnetically compensated interface, the model gives an antiferromagnetic uniaxial anisotropy perpendicular to the magnetization of the ferromagnetic film. There is a rapid transition from perpendicular to parallel anisotropy as the amount of uncompensated moments is increased. The density of uncompensated moments necessary to induce such transition decreases as the interface exchange coupling is reduced. These predictions are compared to the experimentally observed behavior of NiO in various types of interfaces with ferromagnetic materials.

I. INTRODUCTION

A considerable effort has been dedicated to the investigation, with both theoretical and experimental methods, of the magnetic structure at the interface between a ferromagnetic (FM) and an antiferromagnetic (AFM) material. The interest of this topic is also motivated by the fact that the exchange bias effect, consisting in the breaking of time-reversal symmetry obtained upon field cooling in a FM thin layer deposited over an AFM material,[1] depends strongly on the spin structure at the AFM-FM interface.[2-4]

Micromagnetic calculations show that the ground-state configuration of an ideal magnetically compensated AFM-FM interface corresponds to a perpendicular orientation of the bulk FM moments relative to the AFM magnetic easy axis direction.[5] This configuration is stable since the magnetic moments both in the FM and in the AFM layer exhibit a small canting that vanishes away from the interface.[5] These predictions have been experimentally confirmed for several AFM-FM systems showing perpendicular alignment between the AFM and FM easy axes.[6-8] Although the free energy of an ideal AFM-FM interface is expected to be minimized when the local moments across the interface align perpendicularly, there is also clear experimental evidence that the coupling between a FM metal overlayer and the AFM oxide can be collinear.[9-12] NiO-FM interfaces represent a particularly controversial case. While Matsuyama and co-workers claim that the magnetization of thin Fe films deposited on NiO(001) is in plane and perpendicular to the easy axis of the NiO domains,[13] Zhu *et al.*[10] and Ohldag *et al.*[11,12] observe a collinear coupling in, respectively, thin Co-Fe alloy films and Co or Fe layers over a NiO(001) surface. On the other hand, thin NiO epitaxial layers on a Fe(001) magnetic substrate show an in-plane uniaxial anisotropy perpendicular to the Fe magnetization.[14] The origin of these discrepancies might reside in the fact that one or two atomic layers on either side of the AFM-FM interface are partially oxidized or reduced, leading to a certain amount of uncompensated moments that force a parallel coupling with the magnetic moments in the FM partner.[15] In addition, the amount of defects accumulated at the interface and, consequently, the density of uncompensated interface moments might also be heavily influenced by the roughness of the substrate and by the growth sequence and conditions.

Recently, Tsai and co-workers have used Monte Carlo simulations to show that in the case of rough interfaces that are compensated on average there is a transition from collinear to perpendicular alignment of the FM and AFM spins as the temperature is decreased.[16] Similarly, Monte Carlo simulations have also been applied by Nowak *et al.* to describe the AFM-FM interface exchange interaction and give a possible explanation to exchange bias.[17]

In the following, a micromagnetic model based on the Heisenberg Hamiltonian is applied to an AFM-FM interface. In particular, we have chosen the parameters of the model in order to describe the case of antiferromagnetic NiO. The goal is to supply a simple model for a quantitative description of the AFM-FM interface exchange coupling in order to provide guidelines to make general predictions regarding practical experimental cases. This paper presents such an estimate for the crossover from compensated to noncompensated FM-AFM interfaces. For this purpose a simple phenomenological model at zero temperature is applied which, by describing the amount of uncompensated moments by a mean-field approximation, allows to interpolate between these two extremes. In this respect, the results reported in this paper can be viewed as complementary to the work by Tsai *et al.*[16] where the two limit cases of perfectly compensated or uncompensated AFM-FM interfaces are treated.

The interplay between interface exchange coupling, interface uncompensated spins, and long-range magnetic dipole determines the direction of the AFM layer magnetic anisotropy with respect to the FM magnetization. Both types of coupling that are experimentally observed in NiO-FM interfaces are reproduced. The AFM-FM interface proves very sensitive to the presence of uncompensated moments, with a rapid transition from perpendicular to collinear coupling as their density is increased. This rotation of the easy magneti-

zation axis strongly depends on the magnitude of the interface exchange coupling. A lower interface exchange field requires a lower density of uncompensated moments to stabilize a collinear AFM-FM coupling.

II. MODEL

Neglecting the orbital moment contribution to the total magnetic moment of each atom,[18] the Hamiltonian, in reduced units, is

$$\mathcal{H} = \mathcal{H}^{ex} + \mathcal{H}^{mc} + \mathcal{H}^{rand} + \mathcal{H}^{dip} \qquad (1)$$

with

$$\mathcal{H}^{ex} = -\sum_{i<j} J_{ij} \mathbf{m}_i \mathbf{m}_j, \qquad (2a)$$

$$\mathcal{H}^{mc} = \sum_i \mathcal{H}_i^{mc}(\mathbf{m}_i), \qquad (2b)$$

$$\mathcal{H}^{rand} = -\sum_i \mathbf{H}_i^{rand} \mathbf{m}_i, \qquad (2c)$$

$$\mathcal{H}^{dip} = \sum_{i<j} \frac{\mathbf{m}_i \mathbf{m}_j - 3(\mathbf{m}_i \hat{\mathbf{n}}_{ij})(\mathbf{m}_j \hat{\mathbf{n}}_{ij})}{|\mathbf{R}_i - \mathbf{R}_j|^3}. \qquad (2d)$$

$\mathcal{H}^{ex}$ represents the Heisenberg Hamiltonian, with J_{ij} being the exchange coupling between the moments $\mathbf{m}_i$ and $\mathbf{m}_j$ at the atomic sites $\mathbf{R}_i$ and $\mathbf{R}_j$, respectively. $\mathcal{H}_i^{mc}(\mathbf{m}_i)$ in Eq. (2b) is the magnetocrystalline anisotropy Hamiltonian of the ith atom. $\mathcal{H}^{rand}$ accounts for the interaction with random fields $\mathbf{H}_i^{rand}$, which describe the effect of magnetically active impurities and defects, such as interface roughness, uncompensated moments, domain walls, atomic substitutions, and vacancies.[19] In our simulations $\mathbf{H}_i^{rand}$ is assumed to act only on atoms close to the interface. Finally, $\mathcal{H}^{dip}$ is the contribution to the total Hamiltonian due to the magnetic dipole-dipole interactions, with $\hat{\mathbf{n}}_{ij}$ being the unit vector that points in the direction that connects the atoms at the positions $\mathbf{R}_i$ and $\mathbf{R}_j$.

Each local magnetic moment $\mathbf{m}_i$ in the magnetic primitive cell is treated as a classical vector and is allowed to have its own direction but fixed magnitude, in a similar way as in Ref. 5. The orientation of the atomic moments across the AFM-FM interface is calculated using the usual approach of micromagnetics, where each moment experiences a local effective magnetic field $\mathbf{H}_i$ given by the gradient of the Hamiltonian, $\mathbf{H}_i = -\nabla_{\mathbf{m}_i} \mathcal{H}$. The zero-temperature ground state is obtained applying an iteration method. At each iteration, the effective field at each atom is calculated and the atomic magnetic moment is rotated towards the direction of the field.[20] The process is repeated until a self-consistent stationary state is reached, with all the atomic moments pointing parallel to the local field. Since different initial configurations may lead to different self-consistent final states, one must compare the energy of the different stable final states in order to find the ground state. Periodic boundary conditions have been imposed to limit the range of accessible stationary states to those that have the same periodicity in the plane of the film as the unperturbed bulk AFM lattice. Convergence on a multiple magnetic domain structure with walls crossing the interface is thus avoided.

In bulk NiO, $\mathcal{H}^{ex}$ is given by superexchange acting between second-nearest-neighboring Ni atoms through Ni-O-Ni bonds at 180°. In the simulations this is represented by a finite-thickness fcc array of atoms characterized by a second-nearest-neighbor AFM exchange coupling constant J_{AFM}. In the bulk, the Ni moments are ferromagnetically aligned in {111} planes (FM planes), while adjacent FM planes are ordered antiferromagnetically. The Ni moments are parallel to the FM planes. For (111) FM planes the Ni moments can point in any of the three directions equivalent to $[\bar{2}11]$. Considering time-reversal symmetry, this results in 24 degenerate AFM domain orientations. This particular type of collinear order is a consequence of the magnetic dipole-dipole interactions, which are responsible for forcing the Ni moments parallel to the FM planes, and of a 10^{-3} times smaller magnetocrystalline sixfold anisotropy acting in the FM planes.[21] For AFM domains with (111) FM planes, the latter is calculated assuming $\mathcal{H}_i^{mc}(\mathbf{m}_i) = K_{AFM}\sin^2(3\theta)$, with θ being the angle between the $[\bar{2}11]$ direction and the projection of $\mathbf{m}_i$ on the (111) plane. The magnetocrystalline anisotropy is small compared to the magnetic interaction, but it removes the degeneracy between AFM domain orientations parallel to FM planes.

As far as one is interested only in the magnetic structure in the AFM layer, the problem of finding the magnetic configurations that make $\mathcal{H}$ stationary can be greatly simplified by a mean-field approach to the description of the AFM-FM interface.

The influence of the interface on the AFM magnetic structure can be determined once the interface contribution to the local magnetic effective field $\mathbf{H}_i$ acting on each AFM atom is known. At first, let us focus on the short-range exchange interactions of the AFM magnetic moments with interface magnetic impurities and atoms in the FM substrate (the long-range dipolar interactions between AFM and FM atoms at opposite sides of the interface will be treated further below in this section). Since the exchange interaction is significant only for near-neighboring atoms, the contribution $\mathcal{H}_{int}^{ex}$ to the exchange Hamiltonian of atoms at opposite sides of the interface is

$$\mathcal{H}_{int}^{ex} = -\sum_{k,k'} J_{int} \mathbf{m}_{k'}^{FM} \mathbf{m}_k^{AFM}. \qquad (3)$$

J_{int} is the interface exchange coupling and $\mathbf{m}_{k'}^{FM}$ and $\mathbf{m}_k^{AFM}$ are the magnetic moments of FM or AFM atoms, respectively. The indices k and k' indicate pairs of neighboring atoms at opposite sides of the interface. The interaction of the kth AFM interface atom with its FM neighbors (indicated by the index k') and with interface magnetic defects is described by an interface exchange field $\mathbf{H}_k^{ex}$ having the following expression,

$$\mathbf{H}_k^{\text{ex}} = \sum_{k'} J_{\text{int}} \mathbf{m}_{k'}^{\text{FM}} + \mathbf{H}_k^{\text{rand}}. \tag{4}$$

$\mathbf{H}_k^{\text{ex}}$ is completely defined once its spatial Fourier transform is known. Our mean-field approach consists in entering in the simulations only a few spatial frequencies for $\mathbf{H}_k^{\text{ex}}$, namely the ones that satisfy our choice of periodic boundary conditions. In particular, we would like to discuss here the crossover from compensated to noncompensated FM-AFM interfaces. The ideal (001) surface of a fcc AFM such as NiO is perfectly compensated since the surface atoms are equally divided into two populations, one having moments pointing in the opposite direction with respect to the other. The interface interaction between this ideal AFM surface and an infinitely magnetically stiff FM substrate with no defects can be then described by just a constant interface field equal to $\mathbf{H}^{\text{ex}}$ and parallel to the FM magnetization $\mathbf{M}$. On the other hand, the perfectly noncompensated (001) interface is obtained by removing all the AFM interface atoms whose moments point in the same direction. This situation can be simulated by assuming an interface field that vanishes for one population of AFM atoms and remains equal to $\mathbf{H}^{\text{ex}}$ for the other. To interpolate between these two extremes, and to describe the behavior of the AFM magnetic structure for intermediate concentrations of uncompensated moments, we can consider an effective interface field having the following expression,

$$\mathbf{H}_k^{\text{ex}} = \left\{ 1 - \frac{u}{2} \left[1 - \cos(\mathbf{K} \cdot \mathbf{R}_k) \right] \right\} \mathbf{H}^{\text{ex}}, \tag{5}$$

where $\mathbf{R}_k$ is the position of the kth interface AFM atom and $\mathbf{K}$ is a vector parallel to $\mathbf{M}$ chosen so that $\mathbf{H}_k^{\text{ex}}$ satisfies the boundary conditions. The parameter u can thus be viewed as a measure of the density of uncompensated moments: $u=0$ corresponds to an ideal compensated case (zero random fields and constant interface exchange coupling), while $u=1$ is representative of the totally uncompensated interface. In the latter case the interface field vanishes for half the population of interface AFM moments, while for the other half the experienced field is just $\mathbf{H}^{\text{ex}}$.

In principle, other terms could be added to the expression of $\mathbf{H}_k^{\text{ex}}$ to describe, for instance, the presence of interface uncompensated moments noncollinear to $\mathbf{H}^{\text{ex}}$ or the canting of the moments in the FM substrate.[5] However, the results of the model are not qualitatively affected by adding these extra terms, whose influence will be briefly addressed in Sec. III.

Actually, the AFM atoms that can interact with the FM layer via exchange coupling are not just the ones confined in the first layer. While the AFM atoms in the first layer are coupled by direct exchange with the atoms in the FM layer, the AFM atoms in the second layer can interact with the FM substrate via indirect exchange through the oxygen ligands. Moreover, real interfaces are not sharp, since there might be some interdiffusion and partial reduction/oxidation.[12,15] In the simulations, these phenomena are, to some extent, taken into account by introducing two distinct effective exchange fields acting on the first and on the second AFM layer, with magnitude equal to $H_{\text{1st}}^{\text{ex}}$ and $H_{\text{2nd}}^{\text{ex}}$, respectively.

If the FM substrate could be approximated by a continuous distribution of magnetic moments giving a uniform magnetization, the dipolar interaction between FM and AFM atoms would vanish since, in this case, there would be no magnetic field outside the FM layer. In the discrete case, however, this field is not zero and the AFM-FM dipolar interaction should be included in the evaluation of $\mathcal{H}$. For a semi-infinite periodic distribution of FM moments, such as the one imposed by our choice of boundary conditions, the field decays exponentially as a function of the distance from the FM surface, and becomes negligible at a few FM lattice parameters away from it.[22] Such dipolar field can therefore be viewed as an interface contribution and can be accounted for in the definition of $H_{\text{1st}}^{\text{ex}}$ and $H_{\text{2nd}}^{\text{ex}}$ even though it is generally much smaller than the interface exchange field. The directions of the magnetic moments in the AFM film are thus given by the solutions of the Hamiltonian in Eq. (1) restricted to the atoms belonging to just the AFM film, provided that the term $\mathbf{H}_k^{\text{ex}}$ given in Eq. (5) is substituted to $\mathbf{H}_i^{\text{rand}}$ in the expression of $\mathcal{H}^{\text{rand}}$ appearing in Eq. (2c). This approach has the advantage to strongly reduce the number of parameters necessary to model the interface. Let us remember that the orientation of the FM atomic moments near the FM-AFM interface depends in a very complicated way on parameters such as the FM or AFM thickness, exchange coupling, moment magnitude, and anisotropy.[2] The mean-field model described above will instead give results that can be easily generalized to a large variety of cases, providing a guideline to make general predictions regarding the magnetic anisotropy in practical experimental cases. Moreover, we would like to underline that in the model presented above the AFM anisotropy is treated from first principles. In many Monte Carlo simulations, the AFM anisotropy is usually introduced *ad hoc* by assuming that the AFM layer has a uniaxial in-plane anisotropy axis.[16,17] However, the correct description of the AFM anisotropy is crucial if the model is intended to give a reliable picture of the AFM magnetic structure to be compared to real cases.

III. RESULTS AND DISCUSSION

The free parameters in the model are expressed using reduced units. Magnetic moments will be measured in terms of the magnitude m of the magnetic moment on each AFM atom, lengths in terms of a, the lattice constant of the AFM lattice. All magnetic fields will be expressed in units of m/a^3 and energies in terms of m^2/a^3.

The FM magnetization $\mathbf{M}$ is taken parallel to the plane of the interface, to account for shape anisotropy. Qualitatively similar results are obtained if $\mathbf{M}$ points along either the [100] or the [110] direction. Hereafter, the case $\mathbf{M}$ parallel to [110] is discussed, since this is the situation expected for NiO thin films on Fe(001). The easy magnetization axes of iron belongs in fact to the $\langle 100 \rangle$ family, and, in epitaxial thin NiO/Fe(001) films, the fcc NiO lattice is rotated by 45° around the surface normal with respect to the Fe bcc lattice. In our mean-field approach, the direction of $\mathbf{M}$ conditions the choice of the vector $\mathbf{K}$ appearing in Eq. (5), which assumes the value $\mathbf{K} = (\pi/2)(\hat{\mathbf{i}} + \hat{\mathbf{j}})$, $\hat{\mathbf{i}}$ and $\hat{\mathbf{j}}$ being the unit vectors

pointing in the [100] and [010] directions, respectively.

In the present paper, an AFM film composed of ten atomic layers is considered. $\mathcal{H}^{\mathrm{dip}}$ is approximated by evaluating the sum in Eq. (2d) across the entire thickness of the AFM layer, but truncating it in the (100) and (010) directions perpendicular to the film normal to just include the magnetic moments contained in a large cluster surrounding the atom located at $\mathbf{R}_i$. We adopt a $10 \times 10 \times 10$ cubic cluster containing 500 cations. The validity of such approach is discussed in Refs. 23 and 24. Note that, although in three dimensions the summation of $1/r^3$ terms such as those in Eq. (2d) generally diverges logarithmically, for a film of finite thickness the summation converges.[25] Therefore, the truncated summation method certainly provides a good approximation of dipolar energies in thin films.

The AFM dipolar anisotropy per atom is equal to $2h_4 = 28.92m^2a^{-3}$,[21] so K_{AFM} is taken equal to $0.08m^2a^{-3}$ to respect the correct order of magnitude expected for the NiO magnetocrystalline anisotropy. The superexchange coupling J_{AFM} between second-nearest-neighboring AFM atoms is assumed equal to $J_{\mathrm{AFM}}=800a^{-3}$. This value is smaller than the one expected for NiO, where the superexchange has been evaluated about 19 meV,[26] which, in reduced units, corresponds to an energy of about $5400m^2/a^3$ (assuming $m \sim 2\mu_B$ and $a \sim 4$ Å). A smaller value for J_{AFM} has been intentionally chosen to enhance the effects of the long-range dipole-dipole interaction and to reduce the number of iterations necessary for the systems to relax in a stationary state. With the choice of parameters given above, the dipolar and magnetocrystalline interactions just represent a small perturbation of the Hamiltonian in Eq. (1), which is dominated by superexchange. The relevant parameters for the AFM layer then reduce just to u, $H_{\mathrm{1st}}^{\mathrm{ex}}/mJ_{\mathrm{AFM}}$ and $H_{\mathrm{2nd}}^{\mathrm{ex}}/mJ_{\mathrm{AFM}}$.

Spin arrangements corresponding to any of the 24 bulk NiO domains are used as initial states at the beginning of the iteration series. All lead to different self-consistent (meta)-stable states. The dipole-dipole interaction introduces the AFM equivalent of shape anisotropy in ferromagnets, favoring the spin configurations where the moments in thin AFM films align close to the in-plane direction.[25,27] For the perfectly compensated interface ($u=0$), the ground state is derived from the configuration with (111) FM planes and moments aligned along the $[\bar{2}11]$ direction or from any of the equivalent configurations that can be obtained from the latter by applying the transformations belonging to the interface symmetry group. There are eight equivalent configurations. Figure 1 shows the orientation of the AFM magnetic moments in the $[\bar{2}11]$-derived ground state with $H_{\mathrm{1st}}^{\mathrm{ex}}=H_{\mathrm{2nd}}^{\mathrm{ex}} =mJ_{\mathrm{AFM}}$, while Fig. 2 shows the layer average magnetization and orientation as a function of the distance from the interface for various combinations of the parameters. The angles between the AFM moments and $\mathbf{M}$ or between the film normal are both much larger than 45°. If all the eight domains equivalent to the one derived from the $[\bar{2}11]$ orientation are equally populated, this leads to the formation of a uniaxial in-plane anisotropy axis perpendicular to the substrate magnetization $\mathbf{M}$.

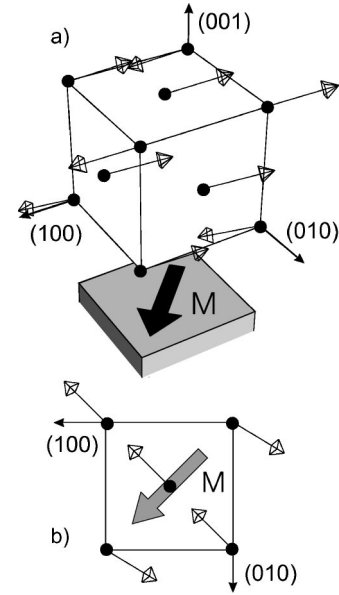The $[\bar{2}11]$-derived configuration is stabilized by a small

FIG. 1. (a) Ground-state AFM magnetic moments in the first three interface atomic layers obtained for a perfectly compensated interface ($u=0$) with $H_{\mathrm{1st}}^{\mathrm{ex}}=H_{\mathrm{2nd}}^{\mathrm{ex}}=mJ_{\mathrm{AFM}}=800ma^{-3}$. The shadowed region represents the FM substrate. The direction of the FM magnetization $\mathbf{M}$ is indicated by the broad arrow. (b) Top view of the magnetic moments in the AFM layer at contact with the FM substrate. The broad arrow represents the FM magnetization $\mathbf{M}$.

canting of the moments, which gives origin to a small net magnetization in the AFM film that rapidly decreases with the distance from the interface. This magnetization varies linearly with the magnitude of the mean interface exchange field. Since a positive value of J_{AFM} has been considered, the moments in the first layer cant away from $\mathbf{M}$, as evident in the lower panel of Fig. 1. The moments tend to slowly rotate towards the direction expected for bulk AFM domains as the distance from the interface is increased. In the calculations, no exchange bias is present and the time-reversal symmetry still holds, thus reversing the sign of J_{AFM} leads to the same self-consistent configuration provided that $\mathbf{M}$ is reversed as well.

Even and odd layers behave almost independently, as one can see from Fig. 2. This depends on the fact that these layers only interact via the weak magnetic dipole-dipole Hamiltonian, since the exchange interaction in the AFM has been assumed to couple only second-nearest neighbors. It must be reminded that the ground state of the dipolar Hamiltonian $\mathcal{H}^{\mathrm{dip}}$ for an AFM system is highly degenerate and the orientations of the simple-cubic AFM sublattices can easily rearrange without loss of dipolar energy.[21] For these reasons, in the following we can assume $H_{\mathrm{2nd}}^{\mathrm{ex}}=0$ without loss of generality.

Figure 3 shows the dependence on the number of uncompensated interface moments of the energy and direction of the $[\bar{2}11]$- and $[211]$-derived configurations for $H_{\mathrm{1st}}^{\mathrm{ex}} =mJ_{\mathrm{AFM}}$ and $H_{\mathrm{2nd}}^{\mathrm{ex}}=0$. The energies of these configurations decrease with u and cross at $u=0.12$. At this value, a reorientation of the in-plane AFM anisotropy axis from perpen-
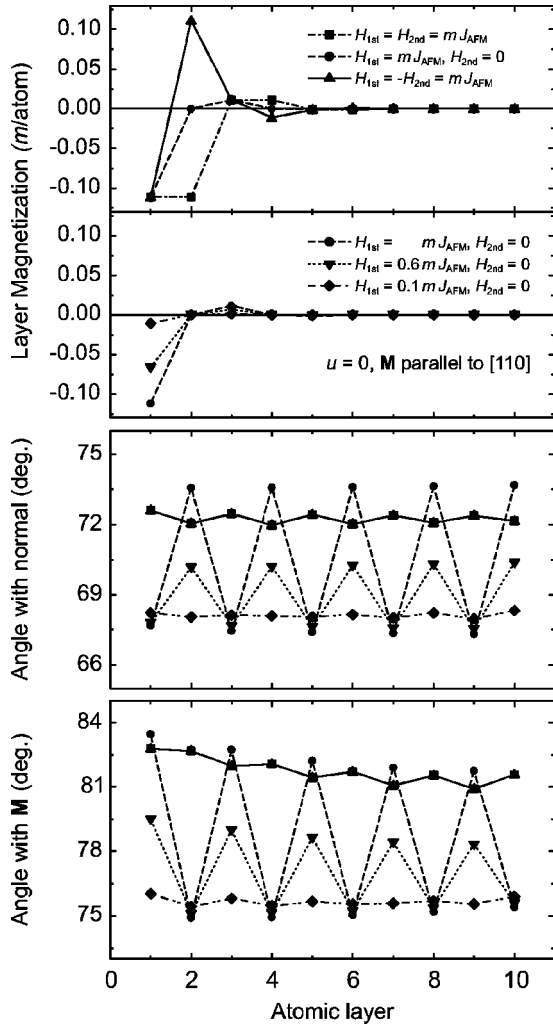
FIG. 2. Layer dependence of the magnetization and of the direction of the magnetic moments in the AFM layer for a magnetically compensated AFM-FM interface ($u=0$). Same symbols in the four panels correspond to curves obtained for same pairs of H_{1st}^{ex} and H_{2nd}^{ex} values.

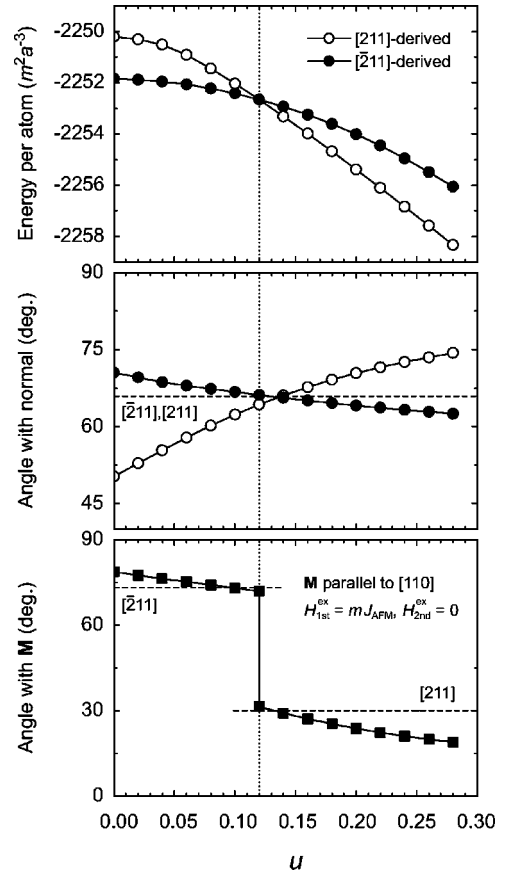FIG. 3. Energy per atom (top panel) and average angle with respect to the film normal (central panel) in the $[211]$-derived and in the $[\bar{2}11]$-derived self-consistent stationary states as a function of the density of uncompensated moments (see text). Bottom panel: average angle between the FM magnetization **M** and the AFM moments in the ground state. The vertical dotted line indicates the value of the parameter u for which the $[211]$-derived and the $[\bar{2}11]$-derived configurations are degenerate. The horizontal dashed lines represent the angles with respect to the indicated directions. The figure refers to the $H_{1st}^{ex}=mJ_{AFM}$, $H_{2nd}^{ex}=0$ case.

dicular to collinear to **M** occurs. It is interesting to note that the two configurations became degenerate when the interaction with the substrate causes the canting of the moments to vanish. This is understandable, since the canting stabilizes one configuration with respect to the other. In the $[211]$-derived ground state the average angle of the moments with respect to **M** is smaller than in the corresponding bulk domain, while in the $[\bar{2}11]$-derived ground state the angle is larger, as already observed in Fig. 2. The two configurations reported in Fig. 3 derive from bulk orientations that have the same projection perpendicular to the film plane, so the vanishing of the canting at the transition implies that the average normal component of the moments does not show a large discontinuity when the anisotropy axis rotates.

Figure 3 illustrates the case of an AFM film on an infinitely stiff FM substrate, where canting of the FM moments is not allowed. In fact, the expression of the interface effective exchange field given in Eq. (5) does not include any term perpendicular to **M**. Let us now study the effects of FM canting, which can be described by adding noncollinear oscillating terms to the right-hand side of Eq. (5). It is significant to evaluate the first-order correction introduced by these extra terms to the energy of the $[\bar{2}11]$- and $[211]$-derived spin configurations when they would be, without FM canting, degenerate. The calculation is straightforward since in this case both the $[\bar{2}11]$- and $[211]$-derived configurations would display a vanishing canting of the AFM moments. One finds that the $[\bar{2}11]$-derived spin arrangement is stabilized with respect to the $[211]$-derived configuration with an energy gain equal to $2.76rm^2a^{-3}$ per atom, with $r=H_{canting}^{ex}/H_{1st}^{ex}$, $H_{canting}^{ex}$ being the component of the interface effective exchange field perpendicular to **M**. Thus, for the same values of H_{1st}^{ex}, H_{2nd}^{ex}, and mJ_{AFM}, the value of the parameter u necessary to induce the transition from perpendicular to collinear AFM-FM coupling should be slightly higher than the one indicated in Fig. 3. Assuming $r\sim0.1$, from Fig. 3 it can be reasonably deduced that the transition would occur when $u\sim0.14$.
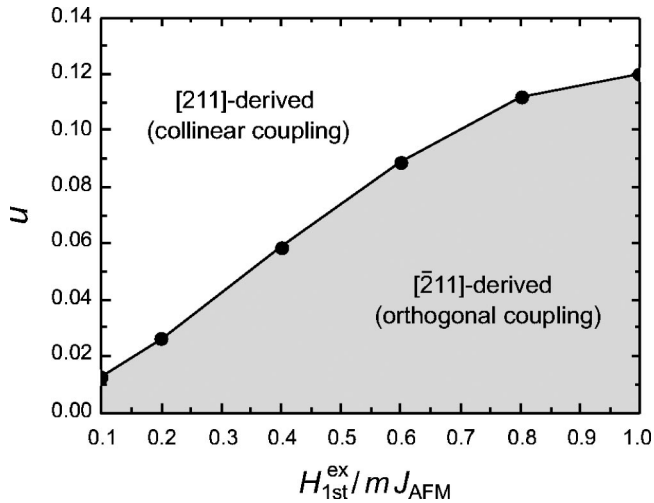
FIG. 4. Diagram describing the regions in the parameter space for which the ground state is derived from either $[211]$ (resulting in collinear AFM-FM coupling) or $[\bar{2}11]$ configurations (corresponding to orthogonal coupling). The diagram refers to the $H_{2nd}^{ex}=0$ case.

The regions in the parameter space for which the ground state is derived from either $[211]$ (resulting in collinear AFM-FM coupling) or $[\bar{2}11]$ domains (corresponding to orthogonal coupling) are shown in Fig. 4 for an infinitely stiff FM substrate. Allowing for FM canting would result in pushing the line dividing the two regions towards slightly higher u values. This effect would be partly counterbalanced by the fact that the canting reduces the component of the FM moments parallel to **M** and, consequently, the H_{1st}^{ex} value. Note, in fact, how the number of uncompensated moments necessary to produce a rotation of the anisotropy axis drastically decreases as the interface exchange field is reduced. Both the experimentally observed types of coupling, orthogonal or collinear, can be reproduced by the model for many combinations of the interface exchange field and uncompensated moments' density. The opposite behavior observed in Fe/NiO bilayers[11] and in the specular case of NiO/Fe interfaces[14] can thus be interpreted, on one hand, as a consequence of a different number of defects induced by different surface roughness, sequence of deposition, and growth conditions. The importance of roughness and uncompensated moments has indeed been pointed out by previous theoretical[16,17] and experimental[12,28] works. Moreover, in FM/AFM interfaces the FM overlayer breaks up in a multidomain magnetic structure reflecting the underlying distribution of AF domains, while a thin AFM layer can be grown on top of a FM substrate that can be magnetized at remanence and made a single magnetic domain. Frustration at the domain walls and magnetic defect density both in the AFM and in the FM material can thus be quite different in the two cases.

On the other hand, however, one can see from Fig. 4 that the rotation of the AFM anisotropy axis might also be induced by a reduction of H^{ex} even if the density of defects remains constant. In a FM/AFM interface the FM layer is typically very thin and the interface exchange coupling with the AF substrate might be reduced with respect to the case of a AFM film on a thick FM material. First, the Curie temperature of a thin FM film rapidly decreases with the film thickness. Second, the disorder of the interface FM moments also depends on the FM anisotropy, which is smaller in thin films.[29] Interface disorder can indeed have the same effects as a reduction of the interface coupling.[17] In both cases the FM magnetization and thus the interface exchange field are reduced with respect to the values that might be expected for the bulk. Luches *et al.* have observed a rapid reduction of the Fe magnetization in iron deposited as a thin film on three atomic layers of NiO when the Fe thickness is decreased below ten atomic layers.[30] The conclusion is that, as far as the coupling with an AFM counterpart is concerned, FM thin films are much more sensitive to interface defects.

IV. SUMMARY AND CONCLUSIONS

A micromagnetic model accounting for exchange, dipolar, and magnetocrystalline interactions has been applied to simulate the magnetic structure of antiferromagnetic films on a ferromagnetic substrate. Although in this paper the model has been applied to NiO, the results of the calculations can be equally well extended to other low anisotropy antiferromagnets, such as MnO and MnF_2. As a consequence of the small single-ion magnetocrystalline anisotropy, the long-range magnetic dipole-dipole interaction forces the AFM moments to preferentially align away from the film normal. Interface exchange interaction with the FM film then induce a uniaxial in-plane anisotropy in the AFM layer. The model reproduces both types of coupling, either orthogonal or collinear, experimentally observed in FM-NiO interfaces between the FM magnetization and the AFM anisotropy axis. The coupling depends strongly on the interface exchange field and on the amount of uncompensated moments at the interface. It is perpendicular for the fully compensated case, but rapidly becomes collinear as the density of uncompensated moments at the interface is increased. A smaller number of defects is required as the interface exchange field is reduced.

*Electronic address: marco.finazzi@fisi.polimi.it

[1] W.H. Meiklejohn and C.P. Bean, Phys. Rev. **102**, 1413 (1956); **105**, 904 (1957).

[2] J. Noguès and I.K. Schuller, J. Magn. Magn. Mater. **192**, 203 (1999).

[3] A. E Berkowitz, K. Takano, J. Magn. Magn. Mater. **200**, 552

(1999).

[4] M. Kiwi, J. Magn. Magn. Mater. **234**, 584 (2001).

[5] N.C. Koon, Phys. Rev. Lett. **78**, 4865 (1997).

[6] Y. Ijiri, J.A. Borchers, R.W. Erwin, S.-H. Lee, P.J. van der Zaag, and R.M. Wolf, Phys. Rev. Lett. **80**, 608 (1998).

[7] T.J. Moran, J. Noguès, D. Ledermann, and I.K. Shuller, Appl. Phys. Lett. **72**, 617 (1999).

[8] J. Noguès, L. Morellon, C. Leighton, M.R. Ibarra, and I.K. Schuller, Phys. Rev. B **61**, R6455 (2000).

[9] F. Nolting, A. Scholl, J. Stöhr, J.W. Seo, J. Fompeyrine, H. Siegwart, J.-P. Locquet, S. Anders, J. Lüning, E.E. Fullerton, M.F. Toney, M.R. Scheinfein, and H.A. Padmore, Nature (London) **405**, 767 (2000).

[10] W. Zhu, L. Seve, R. Sears, B. Sinkovic, and S.S.P. Parkin, Phys. Rev. Lett. **86**, 5389 (2001).

[11] H. Ohldag, A. Scholl, F. Nolting, S. Anders, F.U. Hillebrecht, and J. Stöhr, Phys. Rev. Lett. **86**, 2878 (2001).

[12] H. Ohldag, T.J. Regan, J. Stöhr, A. Scholl, F. Nolting, J. Lüning, C. Stamm, S. Anders, and R.L. White, Phys. Rev. Lett. **87**, 247201 (2001).

[13] H. Matsuyama, C. Haginoya, and K. Koike, Phys. Rev. Lett. **85**, 646 (2000).

[14] M. Finazzi, M. Portalupi, A. Brambilla, L. Duò, G. Ghiringhelli, F. Parmigiani, M. Zacchigna, M. Zangrando, and F. Ciccacci, Phys. Rev. B (to be published).

[15] T.J. Regan, H. Ohldag, C. Stamm, F. Nolting, J. Lüning, J. Stöhr, and R.L. White, Phys. Rev. B **64**, 214422 (2001).

[16] S.-H. Tsai, D.P. Landau, and T.C. Schulthess, J. Appl. Phys. **93**, 8612 (2003).

[17] U. Nowak, K.D. Usadel, J. Keller, P. Miltényi, B. Beschoten, and G. Güntherodt, Phys. Rev. B **66**, 014430 (2002); U. Nowak, A. Misra, and K.D. Usadel, J. Magn. Magn. Mater. **240**, 243 (2002).

[18] In NiO, the Ni orbital magnetic moment is about 15% of the total moment. See V. Fernandez, C. Vettier, F. de Bergevin, C. Giles, and W. Neubeck, Phys. Rev. B **57**, 7870 (1998).

[19] X. Illa, E. Vives, and A. Planes, Phys. Rev. B **66**, 224422 (2002).

[20] R.E. Camley, Phys. Rev. B **35**, 3608 (1987); R.E. Camley and D.R. Tilley, *ibid.* **37**, 3413 (1988).

[21] F. Keffer and W. O'Sullivan, Phys. Rev. **108**, 637 (1957).

[22] J. D. Jackson, *Classical Electrodynamics* (Wiley, New York, 1975), p. 68.

[23] J.A. Sauer, Phys. Rev. **57**, 142 (1940).

[24] J.M. Luttinger and L. Tisza, Phys. Rev. **70**, 954 (1946).

[25] M. Finazzi and S. Altieri, Phys. Rev. B **68**, 054420 (2003).

[26] R.E. Dietz, G.I. Parisot, and A.E. Meixner, Phys. Rev. B **4**, 2302 (1971).

[27] S. Altieri, M. Finazzi, H.H. Hsieh, H.J. Lin, C.T. Chen, T. Hibma, S. Valeri, and G.A. Sawatzky, Phys. Rev. Lett. **91**, 137201 (2003).

[28] J. Camarero, Y. Pennec, J. Vogel, S. Pizzini, M. Cartier, F. Fettar, F. Ernult, A. Tagliaferri, N.B. Brookes, and B. Dieny, Phys. Rev. B **67**, 020413 (2003).

[29] P.J. Jensen and H. Dreyssé, Phys. Rev. B **66**, 220407 (2002).

[30] P. Luches *et al.* (unpublished).